Photochemistry in a dense manifold of electronic states: Photodissociation of CH_2ClBr

Rosendo Valero[1,a)] and Donald G. Truhlar[2,a)]
[1]*Department of Chemistry, University of Coimbra, Coimbra, Portugal*
[2]*Department of Chemistry and Supercomputing Institute, University of Minnesota, Minneapolis, Minnesota 55455-0431, USA*

(Received 29 April 2012; accepted 9 August 2012; published online 14 September 2012)

We report electronically nonadiabatic dynamics calculations including spin–orbit coupling for the photodissociation of CH_2ClBr to yield $Cl(^2P_{3/2})$, $Cl(^2P_{1/2})$, $Br(^2P_{3/2})$, and $Br(^2P_{1/2})$. The potential energy is a 24 × 24 matrix (divided up here into four 6 × 6 blocks in a first approximation to the problem), in a spin-coupled fully diabatic representation obtained by combining the spin-free fourfold way with single-center spin–orbit coupling constants. The spin-free calculations are carried out by multiconfiguration quasidegenerate perturbation theory, and the fully diabatic potentials including spin–orbit coupling are fit to a matrix reactive force field. The dynamics are carried out by the coherent switches with decay of mixing method in the diabatic representation. The results show qualitative agreement with experiment. © *2012 American Institute of Physics*. [http://dx.doi.org/10.1063/1.4747704]

I. INTRODUCTION

Theory has made great progress in understanding electronically adiabatic processes by taking advantage of the Born-Oppenheimer approximation[1] to separate electronic and nuclear motion. Electronically nonadiabatic processes involving two or three electronic states provide the next level of difficulty, and again considerable progress has been made. One often carries out calculations on electronically nonadiabatic processes by using what has been called a "generalized Born-Oppenheimer approximation"[2,3] in which one expands[2–5] the total wave function in N fixed-nuclei electronic eigenfunctions ϕ_j:

$$\Psi = \sum_{j=1}^{N} \psi_j(\mathbf{R})\phi_j(\mathbf{r}, \mathbf{R}), \tag{1}$$

where $\mathbf{R}$ and $\mathbf{r}$ denote, respectively, the nuclear and electronic coordinates, and $\psi_j(\mathbf{R})$ is an expansion coefficient, which also serves as a nuclear wave function for nuclear motion in electronic state j. This may be called the Born-Oppenheimer representation[2,3] or the adiabatic representation.[2,3,5,6]

The adiabatic representation leads to coupled differential equations for the ψ_j where the coupling terms are matrix elements proportional to[2,3,7]

$$\vec{F}_{ij} = -\hbar i \langle \phi_j(\mathbf{r}, \mathbf{R}) | \vec{\nabla}_{\mathbf{R}} | \phi_k(\mathbf{r}, \mathbf{R}) \rangle_{\mathbf{r}} \tag{2}$$

and

$$G_{ij} = -\frac{\hbar^2}{2\mu} \langle \phi_j(\mathbf{r}, \mathbf{R}) | \nabla^2_{\mathbf{R}} | \phi_k(\mathbf{r}, \mathbf{R}) \rangle_{\mathbf{r}}, \tag{3}$$

where $\langle \, . \, \rangle_{\mathbf{r}}$ denotes an integral over $\mathbf{r}$, and $\vec{\nabla}_{\mathbf{R}}$ is the gradient operator. Note that $\mathbf{R}$, $\vec{\nabla}_{\mathbf{R}}$, and $\vec{F}_{jk}$ are all $3N_A$-dimensional vectors, where N_A is the number of atoms in the system, and we scale all nuclear coordinates to a common reduced mass μ. (There is no universal convention for the integral prefactors in Eqs. (2) and (3) so we chose them here to make $\vec{F}_{ij}$ a matrix element of the nuclear generalized momentum and G_{ij} a matrix element of the nuclear kinetic energy.) In a semiclassical approximation in which the electrons are treated quantum mechanically but nuclear motion is treated by classical mechanics, the nuclei move on potential surfaces given by

$$V_j = \langle \phi_j(\mathbf{r}, \mathbf{R}) | H_{\rm el}(\mathbf{r}, \mathbf{R}) | \phi_j(\mathbf{r}, \mathbf{R}) \rangle_{\mathbf{r}}, \tag{4a}$$

where

$$H_{\rm el} = H(\mathbf{r}, \mathbf{R}) - \frac{\hbar^2}{2\mu} \nabla^2_{\mathbf{R}}. \tag{4b}$$

Here H is the total Hamilton of the molecule, and $H_{\rm el}$ is called the electronic Hamiltonian (although it includes nuclear repulsion). The V_j are called the adiabatic potential energy surfaces, and motion on surfaces V_j, V_k, ... is coupled by $\vec{F}_{jk}$ and G_{jk}. This may be accomplished by trajectory surface hopping[8] (TSH) or by various time-dependent self-consistent-field[3] (TDSCF) methods.

A difficulty with the above procedures is that V_j has discontinuous first derivatives and the $\vec{F}_{jk}$ are singular at conical intersections,[9] which occur readily along high-dimensional seams[10,11] ($3N_A - 7$ or $3N_A - 8$ dimensions respectively for states of the same or different symmetry in the absence of spin-orbit coupling[10] or $3N_A - 11$ dimensions for systems with an odd number of electrons when spin-orbit coupling is included[3,12]).

To avoid the complexity of potential energy surfaces with cuspidal ridges coupled by singular vectors, one may transform to a diabatic representation (technically one should say "quasidiabatic," but since "strictly diabatic representations"[2] do not exist,[13–15] there is no confusion in just saying

a)Email addresses: rosendo.valero@gmail.com, truhlar@umn.edu.

"diabatic"). In a diabatic representation the potential energy surfaces, now called U_j, are smooth, and they are coupled by smooth scalars, U_{jk}, which are the now-nonzero off-diagonal elements of the potential energy matrix (with the U_j being the diagonal elements).

The next level of difficulty in molecular dynamics is the case of nonadiabatic processes when there is a dense manifold of coupled electronic states, not just two or three. That is the case considered in the present article. In this case, working in an adiabatic representation becomes even more undesirable, both because of the considerably higher probability of intersections and because adiabatic states are expected to be less physically meaningful (they do not provide a particularly good zero-order picture). Furthermore, TSH methods could involve so many hops that the resulting trajectories would be unphysically jagged and furthermore would require an impractically small step size. Therefore there is a very high motivation to treat the problem by TDSCF methods in a diabatic representation, and this is the approach that we take here. In particular, we use the fourfold way[16–19] to transform to a diabatic representation and the coherent switches with decay of mixing (CSDM) method,[21–25] which is a TDSCF method, to propagate the trajectories. These methods are well suited to be used together because CSDM is about equally accurate in diabatic and adiabatic representations, unlike TSH, which is on average much more accurate in an adiabatic representation than in a diabatic one.

The system under consideration in the present article is photodissociation of CH_2ClBr, which can yield CH_2Br with Cl or Cl^* or CH_2Cl with Br or Br*, where an asterisk denotes electronic excitation, in particular production of the spin-orbit-excited $^2P_{1/2}$ state of the halogen rather than the ground $^2P_{3/2}$ state. (Note that the absence of an asterisk implies the ground electronic state, and also note that we will not consider energies high enough for the photoexcited species to dissociate to an electronically excited state of either of the organic radicals.) Tzeng *et al.*[26] and North and coworkers[27,28] studied these reactions by time-of-flight mass spectrometry of the products. Both groups determined the $[Br + Br^*]/[Cl + Cl^*]$ branching ratio and the translational energy distributions of the products. North and coworkers also measured anisotropy parameters and the $[Br^*]/[Br]$ branching ratio. Lee *et al.*[29] and Zhou *et al.*[30] performed better resolved experiments by employing imaging methods. Zhou *et al.*[30] rationalized their results in terms of five potential energy surfaces. The reaction has also served as a system for studying the possibility of changing the branching ratios by using shaped laser pulses.[31–33]

The photodissociation of CH_2ClBr has also been studied theoretically. The excited states are repulsive and would be expected to lead to direct dissociation. Takayanagi and Yokoyama[34] used a two-dimensional model with two diabatic surfaces based on configuration interaction with single excitations (CIS) without spin-orbit coupling and predicted that photodissociation would be statistical because of strong diabatic coupling. More complete studies were reported by Gonzalez and coworkers. They used multi-state complete active space 2nd order perturbation theory[41] (MS-CASPT2), and we note to make a connection with the work presented below that this is very similar to multi-configuration quasidegenerate perturbation theory[42] (MCQDPT). Gonzalez and coworkers calculated several electronic states without spin-orbit coupling,[35–37] and they carried out dynamics by using a diabatic representation, first with $N = 2$ in one dimension[36] and then with $N = 3$ in two dimensions.[38] Their diabats were obtained by making the diabatic potentials as smooth as possible in the strong interaction region.[38] Their calculated branching ratios depended strongly on excitation energy. In a later study[39,40] they used the same two-dimensional diabatic model to simulate changing the branching ratio by a combination of IR and UV laser pulses. Our own study presented here will include spin-orbit coupling and will involve dynamics in the full 15 dimensions with $N = 24$.

Section II presents the diabatic potential surfaces and couplings. Section III presents the details of the dynamical calculations. Results and discussion are in Sec. IV. Section V has concluding remarks.

II. POTENTIAL ENERGY SURFACES

Diabatic representations are not unique. The transformation to a diabatic representation does not reduce the nuclear momentum coupling of Eq. (2) or the nuclear kinetic energy coupling of Eq. (3) to zero, but the essence of using a diabatic representation is that the residual momentum and kinetic energy couplings are neglected. This is formally justified by the observation that any smooth diabatic transformation that removes the singular coupling at conical intersections makes the residual coupling of the same order of magnitude as the adiabatic-representation coupling in regions of space where the Born-Oppenheimer separation is a good approximation.[2,43]

The fourfold way takes advantage of this flexibility in the definition of a diabatic representation to define the diabatic representation in terms of molecular orbital uniformity and configurational uniformity such that three particularly desirable properties are obtained.[16,17] First, the diabatic electronic states span exactly the same space as the N adiabatic electronic states in Eq. (1). Second, the diabatic states may be directly determined for any nuclear geometry without having to follow a path through nuclear coordinate space, and they do not depend in any way on the choice of a path. Third, the procedure is the same for any molecular system. No assumptions are made about the shape or smoothness of the diabatic potentials.

The fourfold way was originally defined for systems without spin-orbit coupling,[16–18] and it was later[19] extended to include spin-orbit coupling.

The calculation of the singlet diabatic states of CH_2ClBr has been described previously,[19] where we developed a formalism for obtaining a spin-coupled diabatic representation general enough to treat systems where more than one atom with spin–orbit coupling can be released. In the previous study the triplet states were obtained from the singlet states by a valence bond model,[19] but here they are computed just like the singlets. In summary, the adiabatic states without spin-orbit coupling were first calculated for both C–C1 and C–Br dissociations with MCQDPT based on state-averaged

complete active space self-consistent field (SA-CASSCF) calculations with 12 active electrons in 8 orbitals and the 6-31G(d) basis set. The eight active molecular orbitals are as follows:

$$u_1 = \sigma(\text{C–Cl}),$$

$$u_2 = n(\text{Cl}),$$

$$u_3 = n'(\text{Cl}),$$

$$u_4 = \sigma(\text{C–Br}),$$

$$u_5 = n'(\text{Br}),$$

$$u_6 = n(\text{Br}),$$

$$u_7 = \sigma^*(\text{C–Br}),$$

$$u_8 = \sigma^*(\text{C–Cl}),$$

with the six that are occupied at the Hartree–Fock level listed first, and the LUMO and LUMO+1 numbered as 7 and 8. We use the notation n and n' to denote nonbonding p orbitals on the halogens. Note that in Ref. 19 the calculations were analogous to those performed here but were restricted to the SA-CASSCF level.

These calculations were done separately for the singlets and the triplets so they are state averages of six singlets or six triplets (three singlets correlate with $CH_2X + Y$ and three with $CH_2X^* + Y$, and the same for the triplets, where X and Y are Cl and Br). Each of the doublet states (CH_2X and CH_2X^*) of CH_2Br or CH_2Cl combines with the six spin–orbit states of Cl or Br to yield 12 states; eight of them correspond to the halogen in a $^2P_{3/2}$ state, and four correspond to $^2P_{1/2}$. We include both the ground and first excited state of CH_2Br (in the Cl dissociation) or CH_2Cl (in the Br dissociation), which yields a total of 24 states.

A key aspect of MCQDPT is that, like MS-CASPT2, it has qualitatively correct behavior at conical intersections. In both methods this is achieved by making a diagonalization be the last step in calculating the state energies. Both methods include both static correlation, making them well adapted to computing whole potential energy surfaces, and dynamical correlation, which is needed for quantitative accuracy.

First, the fourfold way was used to transform the valence adiabatic states to valence diabatic states for both singlets and triplets, where "valence" is used in the "V-diabatic" notation of Ref. 19 to denote the absence of spin-orbit coupling. The fourfold way requires the specification of reference orbitals, when needed (usually for degenerate nonbonding orbitals) and group lists of prototype diabatic configuration state functions. We used four reference orbitals, corresponding to two nonbonding p orbitals on each halogen atom. To simplify the application of the fourfold way to CH_2ClBr, for the singlets only the singlet V-adiabatic states showing avoided crossings along the reaction coordinate have been included in the diabatization procedure, leaving out those adiabatic states that are separated from the rest in the strong-interaction region. Thus, the ground state and the higher (sixth) V-adiabatic SA-CASSCF states were excluded from the diabatization procedure, and the remaining four V-adiabatic states were included in the fourfold way. In Ref. 19, we found that those excited singlet states that were diabatized (states 2–5) and the corresponding triplet states are dominated by the configuration state functions with the same occupancies of diabatic molecular orbitals, the only difference being in secondary configuration state functions and the spin coupling of the open-shell electrons. The resulting group lists of prototype configuration state functions for each of the valence diabatic states, as required for this first step, are specified in Table I. The important diabatic configuration state functions represent mainly excitations from the nonbonding orbitals of the halogens to the antibonding C–Br and C–Cl σ^* orbitals. We also found that the triplet diabatic couplings between states 2 and 5 are very similar to the couplings between the analogous singlet states.

Then atomic spin-orbit matrix elements were added based on atomic parentage, with Br spin-orbit coupling switched off for geometries in the Cl dissociation region and Cl spin-orbit coupling switched off in the Br dissociation region. Then another transformation yields the fully diabatic ("F-diabatic") potentials that are used for the dynamics. Other details of these steps are given in Ref. 19.

TABLE I. Group lists for prototype configuration state functions for valence diabats.

Singlets	Prototypes[a]	Singlets	Prototypes
2	22222110	4	22122210
	22212120		22112220
	22221201		22122201
	12222111		21221211
3	22221210	5	21222210
	22222101		21222201
	22211220		22122120
	12221211		21212211
Triplets	**Prototypes**	**Triplets**	**Prototypes**
1	22122120	4	22122210
	12222210		22112220
	12222201		22122201
2	22222110		21221211
	22222101	5	21222210
	12222120		21222201
	12221211		22121220
3	22221210		21222111
	22221201	6	22212210
	21222120		22221201
	21221211		22212201
			22122201
			22122102
			12222201

[a]The notation denotes the occupancy of the eight active orbitals in the order that they are listed in Sec. II. Note that there are only six singlet and six triplet "valence" diabats (see text).

Of the 325 off-diagonal elements in the upper triangle of the **U** matrix, all but 26 have a maximum magnitude (at the geometries calculated) below 0.1 eV, and these were just taken as zero. The **U** matrix is symmetric so that yields 52 nonzero off-diagonal elements. This approximation divides the **U** matrix into a relatively sparse matrix of four noninteracting blocks of six states and couplings each, but not all states within each block are coupled among them. The diabatic states and couplings are distributed as follows: states 1, 2, 3, 13, 14, and 15 plus the 1−3, 2−14, 3−14, 3−15, and 13−15 diabatic couplings; states 4, 5, 6, 16, 17, and 18 plus the 4−5, 5−6, 4−16, 6−16, 6−18, 16−17, and 16−18 diabatic couplings; states 7, 8, 9, 19, 20, and 21, plus the 7−8, 8−9, 7−19, 7−20, 9−21, 19−20, 19−21, and 20−21 diabatic couplings; and states 10, 11, 12, 22, 23, and 24, plus the 10−12, 11−23, 12−24, 22−23, 22−24, and 23−24 diabatic couplings. Thus, there is a symmetry in the composition of the groups, in that always three states of the latter group are coupled to the three states of the former group obtained by adding twelve to their order number. This was to be expected, because the numbering is based on the structure of the asymptotic spin-orbit coupling matrices and the diabatic couplings are dominated by spin-orbit coupling (as opposed to valence coupling between the spin-free states).

The 24 diabatic potentials (U_{jj}) and the 26 most important diabatic couplings with $j < k$ (U_{jk}) were fit to analytic functions, which may be considered to be a diabatic "reactive force field" in the usual language, although technically force fields are the negative gradients of potential fields. In particular, we designed the fitting forms for the potential matrix elements by using a combination of flexible fitting functions for the dissociative coordinates, molecular mechanics terms for spectator degrees of freedom, and switching functions to connect analytic expressions that are valid in different regions of coordinate space.

The final expression for the 24 × 24 diabatic potential matrix is written in terms of the coordinates $\boldsymbol{x} = \{r_{Br}, r_{Cl}, r_{H1}, r_{H2}, \theta_{BrCl}, \theta_{BrH_1}, \theta_{BrH_2}, \theta_{ClH_1}, \theta_{ClH_2}, \theta_{H_1H_2}, \alpha^{P1}_{ClH_1}, \alpha^{P1}_{ClH_2}, \alpha^{P1}_{H_1H_2}, \alpha^{P2}_{BrH_1}, \alpha^{P2}_{BrH_2}, \alpha^{P2}_{H_1H_2}, \beta^{P1}_{H_1ClH_2}, \beta^{P1}_{H_2ClH_1}, \beta^{P1}_{H_1H_2Cl}, \beta^{P_2}_{H_1BrH_2}, \beta^{P_2}_{H_2BrH_1}, \beta^{P_2}_{H_1H_2Br}\}$, where r denotes stretches, θ denotes valence angle bendings, α denotes in-plane angles, and β denotes out-of-plane angles. In-plane and out-of-plane angles are appropriate for planar trigonal molecules with the carbon atom as the center atom. The values of the parameters and potentials relative to the reactant CH_2ClBr are indicated with the R superscript, and those relative to the CH_2Cl and CH_2Br product fragments are indicated by the superscripts $P1$ and $P2$, respectively. The diabatic potential matrix is expressed as

$$\boldsymbol{U}(\boldsymbol{x}) = \boldsymbol{V}(r_{Br}, r_{Cl}) + \boldsymbol{I}\,E(\boldsymbol{x}), \tag{5}$$

where $\boldsymbol{V}(r_{Br}, r_{Cl})$ is a sparse matrix of diabatic energies and couplings that depends only on r_{Br} and r_{Cl}, and $E(\boldsymbol{x})$ is a potential term common to all diabats that is based on a molecular mechanics force field. Note that the central C atom has been omitted in the definition of the coordinates **x** for clarity. The diagonal elements $\boldsymbol{V}_{ii}$ are fits to sums of exponentials and Gaussians and products thereof, and the off-diagonal terms were fit to sums of 2-D Gaussians. The molecular mechanics term $E(x)$ is decomposed as follows:

$$\begin{aligned}
E(\boldsymbol{x}) = {} & \sum_{i=1}^{2} V_r^{[H]}(r_{H_i}) + V_r^{[Cl,P1]}(r_{Cl})(1.0 - t_1(r_{Br})) + V_r^{[Br,P2]}(r_{Br})(1.0 - t_1(r_{Cl})) \\
& + \left(V_\theta^{[BrCl]}(\theta_{BrCl}) + \sum_{i=1}^{2} V_\theta^{[BrH]}\left(\theta_{BrH_i}\right) + \sum_{i=1}^{2} V_\theta^{[ClH]}\left(\theta_{ClH_i}\right) + V_\theta^{[HH]}\left(\theta_{H_1H_2}\right) \right) \\
& t_2(r_{Br}, r_{Cl}) \\
& + \left(\sum_{i=1}^{2} V_{ipb}^{[ClH,P1]}(\alpha_{ClH_i}) + V_{ipb}^{[HH,P1]}(\alpha_{H_1H_2}) \right)(1.0 - t_1(r_{Br})) \\
& + \left(\sum_{i=1}^{2} V_{ipb}^{[BrH,P2]}(\alpha_{BrH_i}) + V_{ipb}^{[HH,P2]}(\alpha_{H_1H_2}) \right)(1.0 - t_1(r_{Cl})) \\
& + \left(V_{opb}^{[ClHH,P1]}(\beta_{H_1ClH_2}) + V_{opb}^{[ClHH,P1]}(\beta_{H_2ClH_1}) + V_{opb}^{[ClHH,P1]}(\beta_{H_2H_1Cl}) \right) \\
& (1.0 - t_1(r_{Br})) \\
& + \left(V_{opb}^{[BrHH,P2]}(\beta_{H_1BrH_2}) + V_{opb}^{[BrHH,P2]}(\beta_{H_2BrH_1}) + V_{opb}^{[BrHH,P2]}(\beta_{H_2H_1Br}) \right) \\
& (1.0 - t_1(r_{Cl})) \\
& + V_{r\theta}^{[BrCl]}(\theta_{BrCl}) t_2(r_{Br}, r_{Cl}) + \sum\nolimits_{i=1}^{2} V_{r\theta}^{[BrH]}(r_{Br}, r_{H_i}, \theta_{BrH_i}) t_2(r_{Cl}) + \sum\nolimits_{i=1}^{2} V_{r\theta}^{[ClH]}(r_{Cl}, r_{H_i}, \theta_{ClH_i}) t_2(r_{Br}) \\
& + \left(\sum_{i=1}^{2} V_{\theta\theta}^{[BrCl,BrH]}(\theta_{BrCl}, \theta_{BrH_i}) + \sum_{i=1}^{2} V_{\theta\theta}^{[BrCl,ClH]}(\theta_{BrCl}, \theta_{ClH_i}) \right.
\end{aligned}$$

$$+\sum_{j=1}^{2}\sum_{i=1}^{2} V_{\theta\theta}^{[BrH,ClH]}(\theta_{BrH_i},\theta_{ClH_j})\Bigg)\, t_2(r_{Br},r_{Cl})$$
$$+\sum_{i=1}^{2} V_{\theta\theta}^{[BrH,BrH]}(r_{Br},\theta_{BrH_1},\theta_{BrH_2})t_2(r_{Cl})$$
$$+\sum_{i=1}^{2} V_{\theta\theta}^{[ClH,ClH]}(r_{Cl},\theta_{ClH_1},\theta_{ClH_2})t_2(r_{Br}). \quad (6)$$

The switching functions in Eq. (6) are defined as

$$t_1(r_{Br}) = 0.5\,(1.0 - \tanh\,(3.0\,(r_{Br} - 5.0)))\,, \quad (7)$$

$$t_1(r_{Cl}) = 0.5(1.0 - \tanh\,(3.0\,(r_{Cl} - 5.0))), \quad (8)$$

$$t_2\,(r_{Br}) = \exp\left(-2.0\left(r_{Br} - r_{Br}^{R}\right)\right), \quad (9)$$

$$t_2\,(r_{Cl}) = \exp\left(-2.0\left(r_{Cl} - r_{Cl}^{R}\right)\right), \quad (10)$$

$$t_2(r_{Br},r_{Cl}) = t_2\,(r_{Br})\,t_2\,(r_{Cl})\,. \quad (11)$$

In what follows, the potential energies in the equations are in eV. For the QM part of the diabats the length units are Å, inverse Å, and other powers of Å, and for the molecular mechanics part, they are Å and deg for distances and angles. The units for stretching force constants are mdyne $Å^{-1}$, and for bending force constants they are mdyne Å rad^{-2}. The cross terms involving mixed second derivatives in angles and distance have units of mdyne rad^{-1}. However, the force constants have a prefactor (different for each type of term) so that the final potential energy is in eV. For stretching terms, we have $f_{str} = 6.24$ (mdyne $Å^{-1}$ to eV $Å^{-2}$); for bending terms, including in-plane and out-plane bending terms and bend-bend cross terms, $f_{bend} = 0.0019$ (mdyne Å rad^{-2} to eV deg^{-2}); and for stretch-bend terms, $f_{strbend} = 0.11$ (mdyne rad^{-1} to eV $Å^{-1}$ deg^{-1}). Note the Hooke's law one-half factor in front of the potential energy expressions for the stretch and bending terms (see below).

A. Fitting of diabatic energies and couplings for dissociative coordinates

The values of the stretching coordinates were chosen so as to form a two-dimensional (2D) grid that represents the rupture of either one of the C–Br or C–Cl bonds. For C–Cl in its equilibrium distance ($r_{Cl} = 1.7625$ Å) and for the values of $r_{Cl} = 1.6$ and 2.3 Å, r_{Br} was varied from 1.45 to 5.0 Å; and for C–Br in its equilibrium distance ($r_{Br} = 1.934$ Å) and for the values of $r_{Br} = 1.7$ and 2.5 Å, r_{Cl} was varied between 1.3 and 5.0 Å. A total of 147 points was thus obtained. The molecule always keeps C_S symmetry, but no symmetry restrictions were applied to the MOs in the SA-CASSCF calculations. The 147-point 2D sets of diabatic energies were fitted to the expressions in Eqs. (12)–(14) by means of the GNUPLOT software.

The choice of functional forms for the diabatic energies has been guided by their shape in the 2D space of C–Br and C–Cl coordinates. As the lowest diabat is dominated by a deep minimum close to the CH_2ClBr equilibrium distance, we have chosen a mixed form with purely repulsive terms and Gaussians, with some terms depending on the product $r_{Br}r_{Cl}$ to capture the correlation between the two coordinates. Thus, we used a unique functional form for the lowest diabatic potential:

$$\begin{aligned}
V_{11}^{fit}(r_{Br},r_{Cl}) = {} & C_1\exp(-1.3(r_{Br}-1.4)) + C_2\exp(-1.95(r_{Br}-1.4)) \\
& + C_3\exp(-2.925(r_{Br}-1.4)) + C_4\exp(-2.0(r_{Br}-1.8)^2) \\
& + C_5\exp(-3.0(r_{Br}-1.8)^2) + C_6\exp(-4.0(r_{Br}-1.8)^2) \\
& + C_7\exp(-1.3(r_{Cl}-1.4)) + C_8\exp(-1.95(r_{Cl}-1.4)) \\
& + C_9\exp(-2.925(r_{Br}-1.4)) + C_{10}\exp(-2.0(r_{Cl}-1.8)^2) \\
& + C_{11}\exp(-3.0(r_{Cl}-1.8)^2) + C_{12}\exp(-4.0(r_{Cl}-1.8)^2) + C_{13} \\
& + C_{14}\exp(-1.5(r_{Br}r_{Cl})) + C_{15}\exp(-r_{Br}r_{Cl}) \\
& + C_{16}r_{Br}\exp(-r_{Br}r_{Cl}) + C_{17}r_{Cl}\exp(-r_{Br}r_{Cl}) \\
& + C_{18}r_{Br}^2\exp(-1.5(r_{Br}r_{Cl})) + C_{19}r_{Cl}^2\exp(-3.0r_{CBr}r_{CCl}). \quad (12)
\end{aligned}$$

The diabatic potentials $i = 2, \ldots, 12$ have in general a dissociative shape in both C-Br and C-Cl coordinates, but some shallow minima show up at short internuclear distances. Thus, the functional form is composed mainly of purely repulsive terms but also a product of Morse functions in r_{Br} and r_{Cl} is introduced

$$\begin{aligned} V_{ii}^{fit}(r_{Br}, r_{Cl}) = {} & C_1 \exp(-C_2 (r_{Br} - C_3)) + C_4 \exp(-C_5 (r_{Br} - C_6)) \\ & + C_7 \exp(-C_8 (r_{Cl} - C_9)) + C_{10} \exp(-C_{11} (r_{Cl} - C_{12})) \\ & + C_{13} \exp(-C_{14} (r_{Br} - C_{15})) \exp(-C_{16} (r_{Cl} - C_{17})) \\ & + C_{18} \exp(-C_{19} r_{Br} r_{Cl}) \\ & + C_{20} (1.0 - \exp(-C_{21} (r_{Br} - C_{22})))^2 (1.0 - \exp(-C_{23} (r_{Cl} - C_{24})))^2. \end{aligned} \quad (13)$$

Finally, the expression for the diabatic potentials $i = 13, \ldots, 24$ has a mixed form, with products of functions of Morse and anti-Morse type and powers of them

$$\begin{aligned} V_{ii}^{fit}(r_{Br}, r_{Cl}) = {} & C_1 (1.0 - \exp(-C_2 (r_{Br} - C_3)))^2 (1.0 - \exp(-C_4 (r_{Cl} - C_5)))^2 \\ & + C_6 (1.0 + \exp(-C_7 (r_{Br} - C_8)))^2 (1.0 + \exp(-C_9 (r_{Cl} - C_{10})))^2 \\ & + C_{11} (1.0 - \exp(-C_{12} (r_{Br} - C_{13})))^4 (1.0 - \exp(-C_{14} (r_{Cl} - C_{15})))^4 \\ & + C_{16} (1.0 + \exp(-C_{17} (r_{Br} - C_{18})))^4 (1.0 + \exp(-C_{19} (r_{Cl} - C_{20})))^4 \\ & + C_{21} (1.0 - \exp(-C_{22} (r_{Br} - C_{23})))^6 (1.0 - \exp(-C_{24} (r_{Cl} - C_{25})))^6 \\ & + C_{26} (1.0 + \exp(-C_{27} (r_{Br} - C_{28})))^6 (1.0 + \exp(-C_{29} (r_{Cl} - C_{30})))^6 . \end{aligned} \quad (14)$$

The diabatic couplings have in general a simple shape that resembles a Gaussian in a given (C–Br or C–Cl) coordinate centered at intermediate dissociation distances and with varying height as the other coordinate varies. Thus, we have chosen a product of Gaussians to fit them

$$V_{ij} = C_{ij} \exp(-\alpha_{r_{Cl},ij} (r_{Cl} - r_{Cl,0,ij})^2) \exp(-\alpha_{r_{Br},ij} (r_{Br} - r_{Br,0,ij})^2). \quad (15)$$

The root mean-square deviation (RMSD) of the 2D fits of the diabatic energies is relatively large, and varies between about 0.5 eV and 1.3 eV, with the lowest-energy states having in general a smaller deviation. The errors obtained in the fits could be diminished by adding more functional forms/parameters, but we found that doing so it is difficult to avoid artifacts (namely, negative energies) in regions where no data points are present, in particular, distances shorter than about 1.6 Å for either C–Br or C–Cl. Thus, we have chosen to define relatively few parameters and obtain smooth potential functions with no artifacts. We mention that diabat number 1 still shows negative energies at short distances, but in this case we have kept the functional form due to its good behavior, particularly close to the CH_2ClBr equilibrium distance, and have corrected the negative energies by adding a repulsive term at short distances (see below).

Figure 1 shows fits for diabatic states numbers 2 and 13 along the dissociation coordinates. The first state is representative of repulsive states 2–12, and the second state of states 13–24, which have relatively well-defined minima. Figure 2 shows fits of diabatic couplings for the coupling between states 2 and 13, a relatively small coupling, and the coupling between states 13 and 15, a relatively large coupling. As can be seen, the shape of the fits to diabatic energies and couplings is reasonable and the asymptotic limits are rather well reproduced. Finally, Figure 3 shows the sets of all fitted 24 diabatic energies, and Figure 4 shows the 26 diabatic couplings.

The fits give diabatic potentials that do not all go to the correct asymptotic limits. Therefore, we have enforced the coincidence of all the diabats that correlate with CH_2X + Y (for the notation, see above) with the lowest diabat (Eq. (12)) when either one of the dissociative coordinates reaches 10.0 Å, and for these same conditions, the coincidence of all the diabats that correlate with CH_2X + Y^* with diabat number 3, of all the diabats that correlate with CH_2X^* + Y with diabat number 13, and of all the diabats that correlate with CH_2X^* + Y^* with diabat number 15. First, we calculate the value of the potentials in Eqs. (12)–(14) for such a value of the r_{Br} distance and separately for the same value of the r_{Cl} distance. Let us call the one-dimensional potentials resulting from the choice of this particular value of the C–Br distance $W_{11}(r_{Cl})$ and $W_{ii}(r_{Cl})$, $i = 2, \ldots, 24$. Then we define the following switching function:

$$t_1(r_{Br}) = 0.5(1.0 - \tanh(3.0 (5.0 - r_{Br}))) \quad (16)$$

and correct the dissociative curves to the right asymptotic limits

$$V_{ii}(r_{Br}, r_{Cl}) = V_{ii}^{fit}(r_{Br}, r_{Cl}) + (W_{11}(r_{Cl}) - W_{ii}(r_{Cl})) t_1(r_{Br}) \quad (17)$$

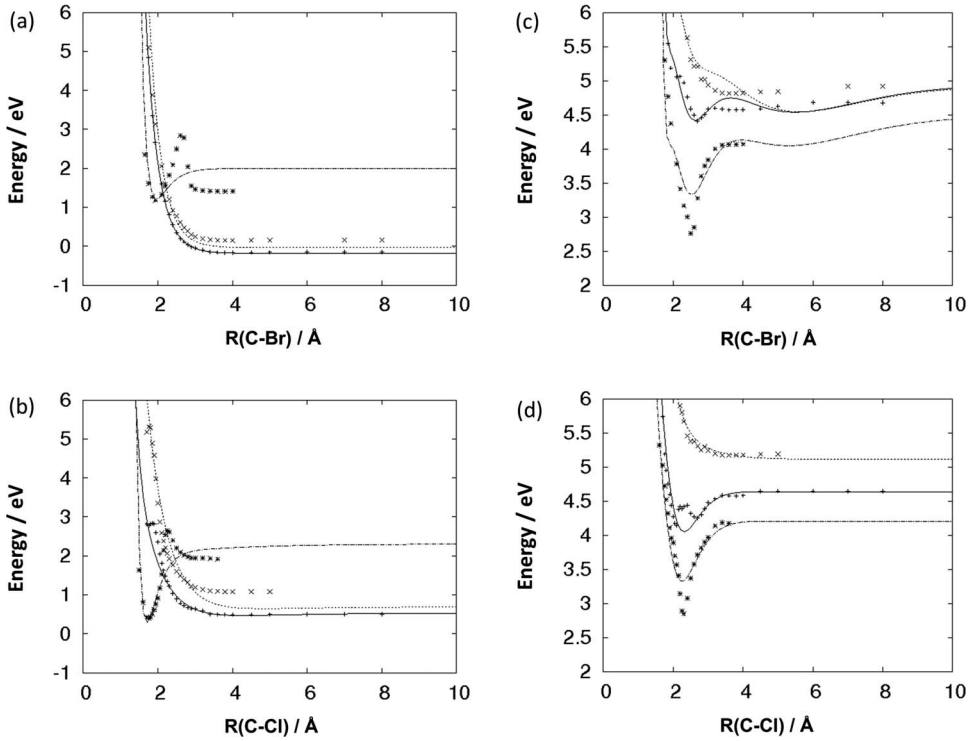

FIG. 1. Fitted and *ab initio* MCQDPT fully diabatic potentials along the dissociation coordinates for photodissociation of CH_2ClBr. (a) State number 2 along the C–Br coordinate; (b) state number 2 along the C–Cl coordinate; (c) state number 13 along the C–Br coordinate; and (d) state number 13 along the C–Cl coordinate. For the C–Br coordinate,$r_{Cl} = 1.7625$ Å (crosses), $r_{Cl} = 1.6$ Å (x-signs), and $r_{Cl} = 2.3$ Å (stars); for the C–Cl coordinate, $r_{Br} = 1.934$ Å (crosses), $r_{Br} = 1.7$ Å (x-signs), and $r_{Br} = 2.5$ Å (stars).

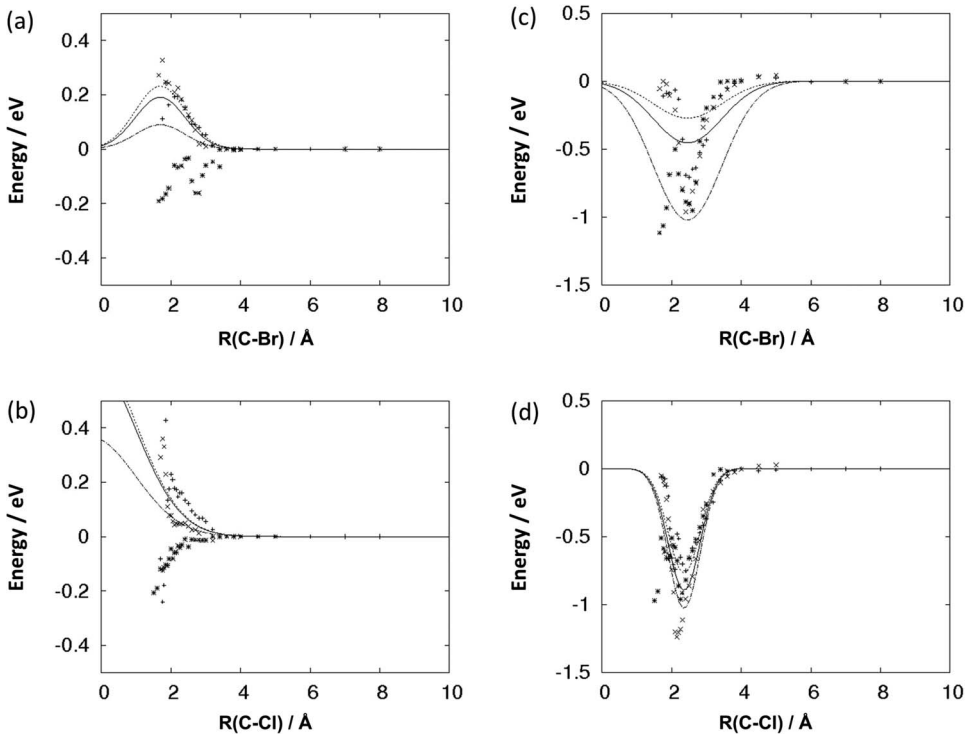

FIG. 2. Fitted and *ab initio* MCQDPT fully diabatic couplings along the dissociation coordinates for photodissociation of CH_2ClBr. (a) Diabatic coupling between states 2 and 13 along the C–Br coordinate; (b) diabatic coupling between states 2 and 13 along the C–Cl coordinate; (c) diabatic coupling between states 13 and 15 along the C–Br coordinate; and (d) diabatic coupling between states 13 and 15 along the C–Cl coordinate. For the C–Br coordinate, $r_{Cl} = 1.7625$ Å (crosses), $r_{Cl} = 1.6$ Å (x-signs), and $r_{Cl} = 2.3$ Å (stars); for the C–Cl coordinate, $r_{Br} = 1.934$ Å (crosses), $r_{Br} = 1.7$ Å (x-signs), and $r_{Br} = 2.5$ Å (stars).

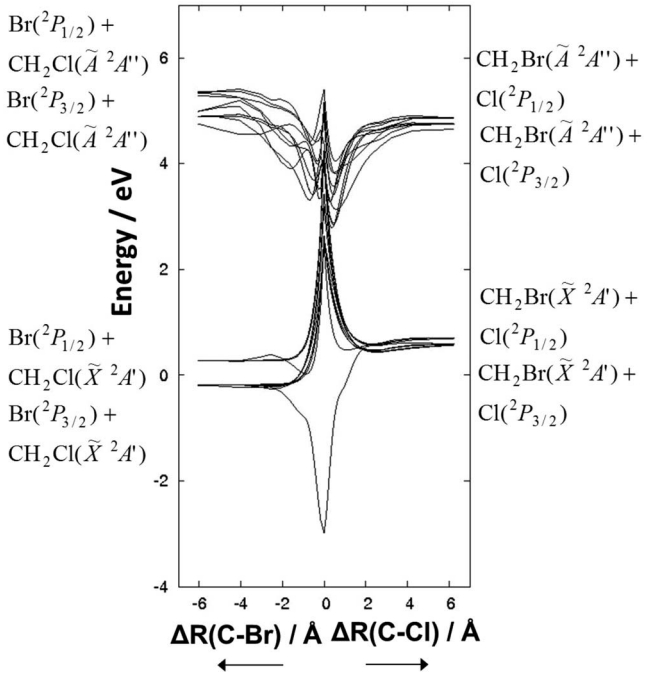

FIG. 3. Fitted 2D MCQDPT fully diabatic potentials along the dissociation coordinates for photodissociation of CH_2ClBr, including the asymptotic corrections in Eqs. (16)–(21). The C–Br and C–Cl bond distances are referenced to the respective equilibrium distances of ground-state CH_2ClBr.

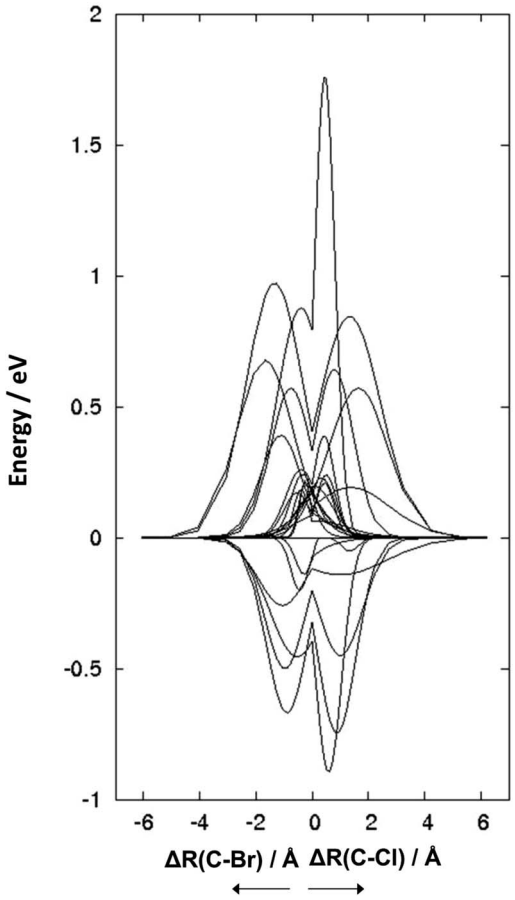

FIG. 4. Fitted 2D MCQDPT fully diabatic couplings along the dissociation coordinates for photodissociation of CH_2ClBr. The C–Br and C–Cl bond distances are referenced to the respective equilibrium distances of ground-state CH_2ClBr.

for the diabatic states that correlate with ground-state bromine atom at dissociation, and

$$\boldsymbol{V}_{ii}(r_{Br}, r_{Cl}) = \boldsymbol{V}_{ii}^{fit}(r_{Br}, r_{Cl}) + (W_{11}(r_{Cl}) - W_{ii}(r_{Cl}) + 0.4569)t_1(r_{Br}) \quad (18)$$

for the diabatic states that correlate with excited-state bromine atom at dissociation, where 0.4569 eV is the value of the spin-orbit splitting of bromine and also the difference between the asymptotic limits of diabats numbers 1 and 3 for ground-state CH_2Cl and of diabats numbers 13 and 15 for excited-state CH_2Cl. Likewise, we define two potentials at a r_{Cl} distance of 10.0 Å, which we call $W_{11}(r_{Br})$ and $W_{ii}(r_{Br})$, $i = 2, \ldots, 24$. We define the switching function

$$t_1(r_{Cl}) = 0.5(1.0 - \tanh(3.0\,(5.0 - r_{Cl}))) \quad (19)$$

and apply it to correct the C–Cl asymptotes as

$$\boldsymbol{V}_{ii}(r_{Br}, r_{Cl}) = \boldsymbol{V}_{ii}^{fit}(r_{Br}, r_{Cl}) + (W_{11}(r_{Br}) - W_{ii}(r_{Br}))\,t_1(r_{Cl}) \quad (20)$$

for the states that correlate with ground-state chlorine atom at dissociation, and

$$\boldsymbol{V}_{ii}(r_{Br}, r_{Cl}) = \boldsymbol{V}_{ii}^{fit}(r_{Br}, r_{Cl}) + (W_{11}(r_{Br}) - W_{ii}(r_{Br}) + 0.1092)t_1(r_{Cl}) \quad (21)$$

for the states that correlate with excited-state chlorine atom, where 0.1092 eV is the value of the spin-orbit splitting of chlorine and also the difference between the asymptotic limits of diabats numbers 1 and 3 for ground-state CH_2Br and of diabats numbers 13 and 15 for excited-state CH_2Br.

The parameters and RMSD of the diabatic energy fits to the expressions in Eqs. (12)–(14) (i.e., before adjusting the asymptotic energies) are shown in Table II. Note that most values of the RMSD are below 1 eV and are generally better for states 1–12, since these states have a simpler shape, with dissociative behavior for most regions of the 2D space, than states 13–24, which show minima at intermediate values of either the C–Br or the C–Cl coordinate and also show some irregularities. This non-smooth behavior is due to the truncation of the electronic space to the lowest six valence singlets and triplets, which eliminates other, higher-energy states that would be important to achieve a smooth diabatization at those energies. We note, however, that this truncation is not expected to affect the dynamics at the total energies we have chosen in this work (see below). One should consider not only the errors in the fits, but the errors in the data fitted, i.e., that MC-QDPT theory itself differs from complete CI. It is hard to estimate the effect of the errors in the fits and the data fitted without repeating the calculations with systematic variations in the analytic potentials, and even doing that exposes one to the well-known inadequacies of sensitivity analysis. This is a general problem not just with the present dynamics calculations based on fits, but also with direct dynamics calculations, where one seldom sees attempts to quantify the effect on the

TABLE II. Parameters of the fits of the dissociative coordinates of the diabatic potential energy surfaces and RMSD values. Units are eV for $C_1 - C_{15}$, eVÅ^{-1} for $C_{16\text{-}17}$, and eVÅ^{-2} for $C_{18\text{-}19}$, for diabatic state 1; eV for C_1, C_4, C_7, C_{10}, C_{13}, C_{18}, C_{20}; Å^{-1} for C_2, C_5, C_8, C_{11}, C_{14}, C_{16}, C_{19}, C_{21}, C_{23}; Å for C_3, C_6, C_9, C_{12}, C_{15}, C_{17}, C_{22}, C_{24}; Å^{-2} for C_{19}, for diabatic states 2–12; and eV for C_1, C_6, C_{11}, C_{10}, C_{16}, C_{21}, C_{26}; Å^{-1} for C_2, C_4, C_7, C_9, C_{12}, C_{14}, C_{17}, C_{19}, C_{22}, C_{24}, C_{27}, C_{29}; Å for C_3, C_5, C_8, C_{10}, C_{13}, C_{15}, C_{18}, C_{20}, C_{23}, C_{25}, C_{28}, C_{30} for diabatic states 13–24.

Diabatic state/ RMSD(eV)	1/0.32	2/0.49	3/1.26	4/0.86	5/0.86	6/0.47	7/0.75	8/0.84
C_1	− 4.976 48	0.332 228	− 2.1847	0.370 991	0.529 323	0.538 514	0.572 729	0.426 713
C_2	− 15.5277	2.3556	1.942 28	2.260 53	2.414 16	2.5138	2.138 85	2.437 02
C_3	21.3448	0.294 632	3.323 94	0.320 671	0.472 033	0.490 549	0.505 904	0.370 503
C_4	10.5668	1.832 28	2.175 26	1.585 95	1.852 46	1.884 47	1.707 52	1.854 62
C_5	− 17.7611	2.963 85	2.137 59	2.357 61	2.320 66	7.866 95	2.384 17	2.500 02
C_6	7.883 59	1.150 09	3.135 05	0.204 235	1.256 51	1.4808	0.656 167	1.228 04
C_7	7.695 88	− 0.655 77	− 0.362 65	− 1.404 37	− 1.365 19	− 2.058 34	− 0.926 28	− 1.915 63
C_8	− 49.1233	0.533 273	1.652 85	0.388 325	0.495 922	1.040 38	0.395 308	1.056 96
C_9	39.5952	0.539 38	− 1.412 51	− 0.612 89	− 0.764 08	2.145 76	0.281 199	1.719 12
C_{10}	− 0.161 96	1.389 18	1.219 64	1.218 26	1.2181	2.150 75	1.292 12	1.995 63
C_{11}	8.885 45	2.936 68	3.604 23	3.609 09	3.609 15	1.328 19	3.3016	1.518 34
C_{12}	− 6.454 83	− 0.475 17	− 1.262 85	− 1.268 91	− 1.269 63	1.906 96	− 0.905 93	1.604 96
C_{13}	3.260 32	1.604 77	1.820 97	1.801 41	1.8005	1.637 44	1.768 98	1.803 22
C_{14}	1267.14	2.906 81	1.942 98	2.211 31	2.308 57	2.569 57	2.278 54	2.463 41
C_{15}	− 781.365	2.085 34	2.228 95	2.075 48	2.067 41	2.102 87	2.079 34	2.0766
C_{16}	152.34	1.840 77	1.744 54	1.686 72	2.000 26	1.527 54	1.636	1.851 14
C_{17}	180.097	1.816 18	2.137 29	2.032 21	2.027 99	1.859 63	1.982 12	2.017 69
C_{18}	− 80.5936	0.904 868	0.831 087	0.972 503	0.941 258	0.495 479	1.106 81	0.340 308
C_{19}	− 1992.26	1.715 49	1.927 22	1.336 57	1.354 19	1.642 46	1.237 24	1.402 83
C_{20}	…	2.923 72	4.784 01	2.675 72	4.293 04	2.767 96	2.663 01	4.015 02
C_{21}	…	3.015 46	3.693 73	4.381 52	1.358 98	3.516 25	4.062 29	1.604 35
C_{22}	…	1.794 81	− 0.615 94	1.795 88	1.7313	1.784 14	1.800 27	1.7316
C_{23}	…	3.415 64	1.595 11	4.630 46	5.315 45	3.994 17	4.719 61	4.835 62
C_{24}	…	1.685 23	1.528 63	1.678 24	1.665 96	1.672 89	1.678 01	1.666 72
C_{25}	…	…	…	…	…	…	…	…
C_{26}	…	…	…	…	…	…	…	…
C_{27}	…	…	…	…	…	…	…	…
C_{28}	…	…	…	…	…	…	…	…
C_{29}	…	…	…	…	…	…	…	…
C_{30}	…	…	…	…	…	…	…	…

Diabatic state/ RMSD(eV)	9/0.51	10/0.95	11/0.49	12/0.85	13/0.69	14/0.87	15/0.95	16/1.21
C_1	− 0.565 81	− 0.908 96	− 0.676 15	− 1.446 96	5.806 68	5.289 63	5.454 56	− 0.506 35
C_2	0.721 093	0.756 647	0.853 719	0.648 619	3.528 38	5.232 91	5.226 58	5.888 57
C_3	0.425 629	0.293 706	0.315 167	1.1341	1.666 21	1.217 99	0.933 162	1.257 81
C_4	1.8913	1.798 53	1.872 55	1.9001	2.925 69	2.727 63	2.726 73	2.741 54
C_5	7.037 87	6.439 07	3.600 06	6.8405	− 1.239 56	− 1.100 42	− 1.098 93	− 1.098 41
C_6	1.591 48	0.477 258	1.4173	1.7083	− 10.2334	− 8.354 07	− 8.219 99	− 12.5873
C_7	− 0.667 75	1.3008	− 0.743 18	− 0.996 49	0.394 592	2.175 22	2.126 54	1.282 15
C_8	0.517 288	2.000 13	0.515 331	0.383 232	2.688 17	1.490 86	1.5405	3.331 18
C_9	0.685 594	0.980 076	0.177 698	0.337 669	2.762 16	1.847 47	1.909 88	1.032 18
C_{10}	1.419 36	1.284 79	1.282 35	1.282 96	− 0.535 22	0.130 364	0.179 629	− 4.188 19
C_{11}	2.675 41	3.269 67	3.274 28	3.279 78	6.148 76	5.496 06	4.603 04	12.6271
C_{12}	− 0.345 56	− 0.870 34	− 0.880 58	− 0.878	1.794 89	1.921 41	1.878 53	2.907
C_{13}	1.647 58	1.723 44	1.694 43	1.724 84	1.983 42	2.013 89	2.049 12	1.823 74
C_{14}	2.440 65	2.6992	2.714 44	1.610 71	6.890 11	6.567 42	6.567 88	14.0317
C_{15}	2.102 22	2.110 17	2.035 96	2.145 36	1.219 61	1.191 36	1.119 73	1.377 57
C_{16}	1.737 42	2.092 59	1.859 36	1.584 61	0.779 861	0.109 629	0.145 688	0.000 402
C_{17}	1.869 51	1.954 12	1.884 35	1.9755	3.102 35	3.643 98	3.644 26	3.528 42
C_{18}	0.630 381	1.000 41	0.893 536	1.057 02	− 0.805 58	− 0.477 97	− 0.476 04	− 0.168 34
C_{19}	1.634 18	1.4356	1.358 54	0.929 687	1.516 18	0.752 162	0.629 422	0.516 963
C_{20}	2.773 25	3.391 35	2.908 94	3.107 18	1.146 03	2.188 28	2.204 68	6.132 01
C_{21}	3.377 18	4.618 53	3.122 13	4.470 64	2.127 35	3.852 07	3.749 86	3.653 81
C_{22}	1.7583	1.788 88	1.783 75	1.740 63	9.842 72	3.134 83	3.245 56	8.788 58
C_{23}	3.933 05	2.321 06	3.497 95	5.106 64	1.554 52	0.943 247	0.968 026	1.567 73

TABLE II. (*Continued.*)

Diabatic state/ RMSD(eV)	9/0.51	10/0.95	11/0.49	12/0.85	13/0.69	14/0.87	15/0.95	16/1.21
C_{24}	1.674 76	1.703 59	1.680 04	1.6661	2.329 45	2.071 17	1.854 48	3.325 78
C_{25}	…	…	…	…	1.675 57	1.708 41	1.591 88	1.607 87
C_{26}	…	…	…	…	0.597 493	0.001 622	0.001 898	0.193 305
C_{27}	…	…	…	…	0.202 074	0.350 858	0.327 494	0.499 163
C_{28}	…	…	…	…	2.549 69	5.457 74	5.639 24	4.024 19
C_{29}	…	…	…	…	1.930 04	5.915 28	5.965 83	6.018 77
C_{30}	…	…	…	…	− 1.477 86	0.945 366	0.735 378	− 0.447 92
Diabatic state/ RMSD(eV)	17/0.97	18/1.11	19/0.96	20/1.28	21/0.58	22/0.97	23/0.85	24/1.33
C_1	4.037 59	2.974 37	− 0.483 58	2.160 17	2.307 23	2.417 09	5.401 52	2.686 36
C_2	1.203 59	1.567 81	5.888 71	1.482 02	5.661 37	1.256 73	5.171 76	2.650 98
C_3	2.390 46	3.898 03	1.259 05	2.027 22	1.6442	2.6361	1.247 39	1.116 51
C_4	3.107 27	2.307 26	2.741 53	2.279	3.179 98	2.434 97	2.746 19	3.828 35
C_5	− 0.213 48	− 0.566 33	− 1.0984	− 0.361 68	− 1.540 96	0.876 346	− 1.112 35	1.996 87
C_6	0.068 838	− 1.232 46	− 12.5529	− 1.113 74	− 9.151 15	− 2.778 49	− 8.310 73	1.357 34
C_7	9.688 99	2.044 49	1.392 33	0.006 969	2.7691	2.091 88	2.187 31	0.729 143
C_8	1.632 75	4.004 61	3.229 18	− 0.434 71	− 1.542 88	− 0.509 21	1.465 57	− 0.645 92
C_9	1.041 82	3.092 91	1.091 92	2.030 21	3.040 96	2.468 82	1.885 99	3.992 14
C_{10}	4.907 16	− 0.817 29	− 4.164 02	− 0.3022	− 1.4812	− 0.3954	0.140 851	1.916 83
C_{11}	5.404 39	0.725 457	12.6296	1.809 67	2.952 26	4.287 09	5.463 08	0.825 78
C_{12}	2.796 07	0.992 482	2.767 68	2.334 94	2.0066	3.378 06	1.919 32	0.782 643
C_{13}	− 0.6022	4.1807	1.821 34	− 0.300 49	1.998 01	1.853 91	2.013 79	2.715 59
C_{14}	2.827 77	2.285 08	14.0293	0.880 217	12.7978	2.861 88	6.368 06	2.728 25
C_{15}	1.635 53	− 1.439 29	1.371 11	1.705 94	1.461 24	− 1.314 44	1.168 01	− 0.584 43
C_{16}	− 3.306 56	0.747 73	0.000 414	1.311 55	− 8.090 71	− 1.945 06	0.135 126	2.235 56
C_{17}	3.452 02	2.418 64	3.529 11	0.952 322	3.707 89	3.032 09	3.626 98	1.587 21
C_{18}	1.616 67	− 0.145 72	− 0.169 77	− 0.773 58	− 0.690 49	1.567 27	− 0.461 69	0.703 051
C_{19}	0.987 536	2.967 76	0.512 937	0.680 266	3.590 91	3.248 15	0.777 104	5.706 82
C_{20}	1.793 45	− 0.042 02	6.126 08	0.576 082	− 1.152 46	− 0.922 97	2.025 57	1.714 31
C_{21}	3.860 37	3.040 96	3.661 59	3.940 99	3.346 37	2.889 72	3.725 48	2.525 09
C_{22}	2.843 76	1.778 03	8.785 07	2.733 89	3.460 43	2.363 85	3.133 07	1.452 11
C_{23}	1.545 55	0.662 408	1.483 85	− 0.820 82	− 1.597 68	− 0.323 68	0.928 752	1.914
C_{24}	2.469 15	1.306 34	3.251 66	2.526 17	2.336 39	2.121 84	2.049 84	3.047 91
C_{25}	1.648 07	1.552 35	1.653 11	1.671 44	1.577 31	1.688 61	1.710 33	1.568 21
C_{26}	0.321 041	1.486 78	0.257 498	1.568 88	14.5571	2.130 12	0.001 265	− 2.279 12
C_{27}	1.847 59	0.898 852	0.550 786	2.668 96	1.273 91	0.961 817	0.342 246	1.511 51
C_{28}	1.727 26	2.758 03	3.717 06	− 0.095 03	− 0.906 66	0.186 959	5.670 71	0.195 232
C_{29}	0.894 49	2.441 02	6.018 47	2.7803	2.671 19	1.4239	5.953 34	4.275 26
C_{30}	1.196 75	− 0.580 67	− 0.446 97	− 0.261 18	0.379 509	0.114 758	0.963 032	1.631 38

dynamics of deviations in the potentials from those that would be obtained with complete configuration interaction. We note, however, that one large contribution to the errors in the fits comes from the repulsive regions of the potentials, where a large error in energy units is less significant when considered in terms of movement of the repulsive walls. Nevertheless, the qualitative agreement we obtained with experiment with these simple fits demonstrates the utility of the method of fitting diabatic potentials with analytic functions based in part on molecular mechanics.

The parameters and RMSD of the diabatic coupling fits to Eq. (15) are shown in Table III. As can be seen, the RMSD oscillates between about 0.1 eV and 0.3 eV, which is much less than for the diabatic energies due to the smaller absolute values of the diabatic couplings and in part also to their simpler shape.

B. Molecular mechanics functions for spectator coordinates

The molecular mechanics functions for CH_2ClBr were either smoothly turned off if they do not exist in the CH_2Br and CH_2Cl products, or they were transformed into those of the products as the dissociative coordinates are stretched. Likewise, potential terms that only exist in products were smoothly turned on as the corresponding asymptote is approached. The parameters of the switching functions are chosen so as to ensure that these conditions are fulfilled, but no attempt was made to fit them to *ab initio* calculations. Full details are given in the supplementary material[61] along with Refs. 44–46 for the MM3 parameters that we used.

The diabatic potentials are shown in Figs. 1–3. In these figures, the C–Br or C–Cl bond is stretched while keeping the other internal coordinates at their equilibrium values.

TABLE III. Parameters of the fits of the diabatic couplings and RMSD values. The diabatic states are designated as i and j. Units are eV for C_{ij}, $Å^{-1}$ for $\alpha_{r_{Cl,ij}}$ and $\alpha_{r_{Br,ij}}$, and Å for $r_{Cl,0,ij}$ and $r_{Br,0,ij}$.

i-j coupling/ RMSD(eV)	1−3/0.29	2−14/0.08	3−14/0.08	3−15/0.11	4−5/0.06	4−16/0.04	5−6/0.06
C_{ij}	1.946 46	0.709 579	0.188 204	2.946 34	0.223 66	22.3827	0.447 982
$\alpha_{r_{Cl,ij}}$	3.852 86	0.296 416	0.406 081	0.178 462	4.530 37	0.262 441	3.788 78
$\alpha_{r_{Br,ij}}$	0.665 365	0.967 806	7.353 76	8.973 56	0.570 027	0.313 824	2.199 55
$r_{Cl,0,ij}$	2.217 46	−0.341 857	1.965 20	−2.086 44	2.211 02	−1.818 39	2.266 61
$r_{Br,0,ij}$	2.322 83	1.689 87	2.322 65	2.187 35	1.576 73	−0.173 108	2.468 79
	6−16/0.04	6−18/0.12	7−8/0.07	7−19/0.04	7−20/0.06	8−9/0.06	9−21/0.08
C_{ij}	1.921 85	2.971 86	−0.326 703	161.519	0.383 843	0.311 042	1.459 58
$\alpha_{r_{Cl,ij}}$	0.148 385	0.098 365 9	5.758 56	0.496 321	−0.176 53	2.236 59	1.248 16
$\alpha_{r_{Br,ij}}$	5.360 610	13.1930	0.979 584	0.642 031	2.280 96	2.811 70	0.179 202
$r_{Cl,0,ij}$	−0.390 605	−3.389 52	2.286 98	−1.686 37	2.271 30	2.096 60	1.847 12
$r_{Br,0,ij}$	−2.734 69	2.179 12	2.537 43	0.746 784	2.082 76	2.266 11	−1.414 04
	10−12/0.08	11−23/0.08	12−24/0.10	13−15/0.23	16−17/0.31	16−18/0.17	19−20/0.30
C_{ij}	0.496 784	1.396 92	8.778 40	−1.030 40	2.026 10	2.342 45	−1.542 59
$\alpha_{r_{CCl,ij}}$	3.570 14	0.220 072	15.4251	2.328 58	0.409 127	0.456 898	1.064 65
$\alpha_{r_{CBr,ij}}$	1.669 34	0.987 532	3.291 38	0.504 797	0.488 274	0.502 407	0.908 972
$r_{Cl,0,ij}$	2.188 17	−1.285 87	1.149 48	2.354 65	3.101 29	3.410 75	2.648 58
$r_{Br,0,ij}$	2.320 02	1.719 88	1.876 28	2.4579	3.272 51	3.609 62	2.827 84
	19−21/0.21	20−21/0.15	22−23/0.18	22−24/0.32	23−24/0.14		
C_{ij}	−1.118 29	−1.514 30	0.634 976	1.105 08	8.791 55		
$\alpha_{r_{CCl,ij}}$	0.785 718	5.328 55	0.253 553	1.066 69	15.4655		
$\alpha_{r_{CBr,ij}}$	0.966 377	8.238 23	0.958 028	0.960 063	4.362 57		
$r_{Cl,0,ij}$	2.773 73	3.119 44	3.144 98	2.550 40	1.185 87		
$r_{Br,0,ij}$	2.904 11	1.300 82	3.052 95	2.687 22	−0.079 045 2		

The molecule thus retains C_s symmetry. The zero of energy is the lowest spin-free asymptotic limit, i.e., $CH_2Cl(\tilde{X}\,^2A') + Br(^2P)$.

The structure and frequencies of the ground state of CH_2ClBr and the ground-state dissociation energy D_0 for producing $CH_2Br + Cl$ or $CH_2Cl + Br$ are given in Table IV. Note the good general agreement of the features of both the reactant CH_2ClBr and the products, which are also situated energetically with good accuracy. Further exploration of the ground-state potential surface has revealed that there exist weekly bound complexes of the form iso-$CH_2X\cdots Y$ where X and Y are either Cl or Br and the halogens make a weak bond with each other. In previous studies, complexes of this kind have been identified, many of them between closed-shell species and halogen atoms,[47–51] but also between the halogen atom and one bound halogen in the remaining radical (e.g., formation of iso-bromoform in the photolysis of bromoform in solution,[52] and formation of iso-chloroiodomethane in the photolysis of chloroiodomethane in cryogenic matrices).[53] We have identified the $CH_2X\cdots Y$ complexes at the MP2/6-311+G(d,p) level of theory, and their geometries and frequencies are also reported in Table IV. Their energies relative to the respective dissociated complexes at the MP2/6-311+G(d,p) level are –15.2 kcal/mol for the $CH_2Br\cdots Cl$ complex and –4.7 kcal/mol for the $CH_2Cl\cdots Br$ complex. It is important to note that CH_2Br and CH_2Cl are planar or quasi-planar according to experiment.[54–56] Thus, we have defined these radical products as planar in our potential form despite them being non-planar at the MP2/6-311+G(d,p) level. We have not included the complexes in our potential form.

III. DYNAMICS CALCULATIONS

The dynamics calculations were carried out by CSDM, which introduces decoherence into the electronic degrees of freedom of a trajectory propagating on a self-consistent potential. We ran 115 trajectories for each total energy and initial state.

The numbering of the diabatic states is based on the spin-orbit coupling matrix; the numbering corresponds approximately to the energetic ordering of the states, but not precisely since the diabats cross each other. The notation 6(Br,Cl), for example, denotes a trajectory beginning in state 6, and the parenthetical is a state that correlates upon dissociation of the C-Br bond with ground-state $Br(^2P_{3/2})$; and upon dissociation of the C-Cl bond it correlates with ground-state $Cl(^2P_{3/2})$. The notation $5(Br^*,Cl^*)$ denotes trajectories that start on state 5, which correlates upon C–Br dissociation with electronically excited $Br(^2P_{1/2})$ and upon C–Cl dissociation with electronically excited $Cl(^2P_{1/2})$. Correlations are as follows: states 1–12 correlate with CH_2X upon dissociation of the C–Y bond, and states 13–24 correlate with CH_2X^*. States 3, 5, 8, 10, 15, 17, 20, and 22 correlate with Y^*; and the other states correlate with Y.

We consider two values of the total energy E, which is defined as the total energy relative to the harmonic zero point vibrational level on the ground adiabatic potential energy surface. Our potential surface yields 0.78 eV for that zero point energy, in good agreement with an *ab initio* value of 0.80 eV calculated by MP2/6-311+G(d,p). The two total energies, 5.0 and 6.4 eV, chosen for study here are equal to the photon energies of two of the experimental studies. Note that a

TABLE IV. Characteristics of the ground adiabatic potential energy surface yielded by electronic structure[a] calculations and by diagonalizing our fitted diabatic potential energy matrix.

	CH_2ClBr geometry		CH_2ClBr frequencies/cm^{-1}		$CH_2Br(\tilde{X}\,^2A') + Cl(^2P_{3/2})$ D_0/eV		$CH_2Cl(\tilde{X}\,^2A') + Br(^2P_{3/2})$ D_0/eV	
	MP2	Fit	MP2	Fit	MCQDPT[a]	Fit	MCQDPT[a]	Fit
R(C-Br)/Å	1.93	1.95	3242	2976	3.37	3.38	2.73	2.82
R(C-Cl)/Å	1.76	1.73	3162	2908				
R(C-H)/Å	1.09	1.09	1469	1511				
< Cl–C–Br	113.5°	113.5°	1310	1358				
<H–C–Cl	108.9°	109.0°	1187	1253				
< H–C–Cl–Br	119.4°	119.3°	879	925				
			794	774				
			639	668				
			238	209				
	CH_2Br geometry		CH_2Br frequencies/cm^{-1}		CH_2Cl frequencies/cm^{-1}			
	MP2	Fit	CASSCF	Fit	CASSCF	Fit		
R(C-Br)/Å	1.85	1.88	3511	3000	3511	3002		
R(C-H)/Å	1.08	1.09	3360	2888	3361	2894		
<H–C–Br	117.6°	117.7°	1513	1535	1540	1677		
< H–C–Br–H	165.9°	180.0°	979	1014	1066	1184		
			659	884	808	1169		
			542	435	470	643		
	CH_2Cl geometry							
	MP2	Fit						
R(C-Cl)/Å	1.70	1.76						
R(C-H)/Å	1.08	1.09						
<H–C–Cl	117.7°	117.8°						
< H–C–Cl–H	169.7°	180.0°						
	$CH_2Br\cdots Cl$ geometry	$CH_2Br\cdots Cl$ frequencies/cm^{-1}	$CH_2Cl\cdots Br$ frequencies/cm^{-1}					
	MP2	MP2	MP2					
R(C-Br)/Å	1.77	3325	3324					
R(Br-Cl)/Å	2.47	3181	3181					
R(C-H)/Å	1.08	1453	1482					
< Cl–Br–C	117.9°	995	1074					
<H–C–Br	117.6°	846	957					
< H–C–Br–Cl	80.4°	739	736					
		507	480					
		303	289					
		167	181					
	$CH_2Cl\cdots Br$ geometry	507	480					
	MP2							
R(C-Cl)/Å	1.64							
R(Cl-Br)/Å	2.54							
R(C-H)/Å	1.08							
< Br–Cl–C	120.1°							
<H–C–Cl	117.1°							
< H–C–Cl–Br	79.4°							

[a]MP2 geometries, MCQDPT energies, and CASSCF(7,5) frequencies.

total energy of 6.4 eV puts us at 4.4 eV on the scale of Fig. 3.

For each total energy E and initial excited diabatic electronic state j considered, we selected initial conditions for the trajectories by the same method as in a previous study of photodissociation of ammonia,[57,58] but here using a Wigner ground-vibrational-state probability distribution for the lowest adiabatic potential energy surface. Each sample of this distribution yields a set of coordinates $\mathbf{R}$ and momenta $\mathbf{P_R}$. Then we calculate

$$E_0 \equiv \frac{\mathbf{P_R^2}}{2\mu} + U_j. \tag{22}$$

If E_0 agrees with E within a tolerance ΔE, we accept the initial conditions $\mathbf{R}$, $\mathbf{P_R}$; if not we take another sample. This procedure generates an excited state distribution

consistent with the Franck-Condon principle. We set ΔE equal to 0.01 eV. Several states have negligible Franck-Condon factors with the ground adiabatic electronic state. Therefore, those states were not considered as initial states in the dynamics.

The trajectories were calculated by the CSDM method in the fully diabatic representation. The fully adiabatic representation that would result from diagonalization of the fully diabatic one cannot be used in the dynamics because extremely small time steps would be required to ensure good energy conservation. The trajectories were propagated with a specially designed variable-time-step integration scheme[59] in the ANT program[60] with an initial time step of 1 fs, which yields good energy conservation (to about 10^{-6} eV for the shortest trajectories and 10^{-2}–10^{-3} eV for the longest ones). Because decoherence is included, each trajectory ends in a definite electronic state.

Because the density of states is high, the number of places where the CSDM algorithm sets the locally coherent density matrix equal to the decay of mixing density matrix[20,25] is also large. This is a mild operation, and so it does not lead to jagged trajectories such as would be generated by frequent surface hops, which have discontinuous momenta (there are no surface hops in CSDM).

IV. RESULTS AND DISCUSSION

At low energy, the Franck-Condon excitation process populates states with a steepest descent path leading to Br or Br^*, whereas at high energy no definite statement can be made.

The trajectories are stopped when either Cl or Br is 10 Å away from CH_2X. At 5 eV, the dynamics is direct with a typical trajectory time of 300–400 fs. At 6.4 eV the states that correlate with CH_2X^* are accessible in the molecular region but not asymptotically; therefore trajectories can get trapped until they relax to one of states 1–12. Some trajectories did not even complete in 20 ps, which is the maximum time allowed by the program; such trajectories are discarded, but this does not have a large effect on the final results because such trajectories constitute only about 0%-5% of the total number.

The results are given in Table V. For comparison we note that the experimental results[26] for $[Br + Br^*]/[Cl + Cl^*]$ is no Cl at 5.0 eV and 4.5 at 6.4 eV, and the experimental results[28] for $[Br^*]/[Br]$ are 0.14 ± 0.10 at 5.0 eV and 0.18 ± 0.10 at 6.4 eV. To compare quantitatively to experiment we would need transition dipole matrix elements to compute correct weights for the various initial states, but we can make some preliminary observations without these.

First, the results are clearly nonstatistical with a strong dependence on photon energy and initial state.

Second, the Br^*/Br branching ratios at 5.0 eV are qualitatively in agreement with experiment, and these ratios at 6.4 eV could be in agreement with experiment, depending on the unknown Franck-Condon factors and transition dipole matrix elements.

Third, the $[Br + Br^*]/[Cl + Cl^*]$ ratio is roughly consistent with experiment at 5.0 eV, predicting a small percentage of total chlorine dissociation, and the ratio could also be consistent with the experiment at 6.4 eV, again depending on the weighting of the different states. It is interesting to note that all the branching ratios of states 1–12 are roughly similar as are those of states 13–24, and the latter are all larger and close to one.

TABLE V. Calculated branching ratios.

Energy (eV)	Initial state	$[Br + Br^*]/[Cl + Cl^*]$	$[Br^*]/[Br]$
5.0	6 (Br/Cl)	28	0.16
	7 (Br/Cl)	56	0.10
	9 (Br/Cl)	37	0.29
	11 (Br/Cl)	56	0.0
	12 (Br/Cl)	no Cl	0.31
6.4	4 (Br/Cl)	3	0.29
	5 (Br^*/Cl^*)	4	1.71
	6 (Br/Cl)	3	0.41
	7 (Br/Cl)	57	0.11
	8 (Br^*/Cl^*)	6	1.9
	9 (Br/Cl)	2	0.25
	10 (Br^*/Cl^*)	4	0.33
	11 (Br/Cl)	5	0.0
	12 (Br/Cl)	6	1.25
	16 (Br/Cl)	1	0.63
	18 (Br/Cl)	1	1.05
	19 (Br/Cl)	1	0.58
	21 (Br/Cl)	1	0.80
	23 (Br/Cl)	1	0.0
	24 (Br/Cl)	1	0.0

V. CONCLUDING REMARKS

Polyatomic systems with a dense manifold of excited electronic states are very important in many applications, but theoretical treatments of such cases have been rare. We have shown here that the fourfold way diabatization scheme and the coherent switches with decay of mixing dynamics method can be used together to carry out electronically nonadiabatic dynamics calculations on a polyatomic system with a dense manifold of electronic states. We find that the dynamics are nonstatistical, and in four comparisons the branching ratios are in qualitative agreement with experiment. Further analysis will require improved potential energy surfaces and couplings and the calculation of Franck-Condon factors and transition dipole matrix elements.

ACKNOWLEDGMENTS

The authors are grateful to Ahren Jasper for helpful assistance. This work was supported in part by the National Science Foundation under Grant No. CHE09-56776.

[1]M. Born and R. Oppenheimer, Ann. Phys. (Leipzig) **389**, 457 (1927).
[2]B. K. Kendrick, C. A. Mead, and D. G. Truhlar, Chem. Phys. **277**, 31 (2002).
[3]For a review, see A. W. Jasper, B. K. Kendrick, C. A. Mead, and D. G. Truhlar, Adv. Ser. Phys. Chem. **14**, 329 (2004).
[4]N. F. Mott, Proc. Cambridge Philos. Soc. **27**, 553 (1931).
[5]M. Born and K. Huang, *Dynamical Theory of Crystal Lattices* (Oxford University Press, London, 1956).
[6]W. R. Thorson, J. Chem. Phys. **34**, 1744 (1961).

[7]J. O. Hirschfelder and W. J. Meath, Adv. Chem. Phys. **12**, 3 (1967).
[8]For a review, see S. Chapman, Adv. Chem. Phys. **82**, 423 (1992).
[9]G. Herzberg, *Molecular Spectra and Molecular Structure III. Electronic Spectra and Electronic Structure of Polyatomic Molecules* (van Nostrand Reinhold, New York, 1966).
[10]E. Teller, Israel J. Chem. **7**, 227 (1969).
[11]D. G. Truhlar and C. A. Mead, Phys. Rev. A **68**, 32501 (2003).
[12]C. A. Mead, J. Chem. Phys. **70**, 2276 (1979).
[13]A. D. McLachlan, Mol. Phys. **4**, 417 (1961).
[14]C. A. Mead and D. G. Truhlar, J. Chem. Phys. **77**, 6090 (1982).
[15]B. K. Kendrick, C. A. Mead, and D. G. Truhlar, Chem. Phys. Lett. **330**, 629 (2000).
[16]H. Nakamura and D. G. Truhlar, J. Chem. Phys. **115**, 10353 (2001).
[17]H. Nakamura and D. G. Truhlar, J. Chem. Phys. **117**, 5576 (2002).
[18]H. Nakamura and D. G. Truhlar, J. Chem. Phys. **118**, 6816 (2003).
[19]R. Valero and D. G. Truhlar, J. Phys. Chem. A **111**, 8536 (2007).
[20]C. Zhu, S. Nangia, A. W. Jasper, and D. G. Truhlar, J. Chem. Phys. **121**, 7658 (2004).
[21]A. W. Jasper, C. Zhu, S. Nangia, and D. G. Truhlar, Faraday Discuss. **127**, 1 (2004).
[22]C. Zhu, A. W. Jasper, and D. G. Truhlar, J. Chem. Theory Comput. **1**, 527 (2005).
[23]W. Jasper, S. Nangia, C. Zhu, and D. G. Truhlar, Acc. Chem. Res. **39**, 101 (2006).
[24]D. G. Truhlar, in *Quantum Dynamics of Complex Molecular Systems*, edited by D. A. Micha and I. Burghardt (Springer, Berlin, 2007), p. 227.
[25]A. W. Jasper and D. G. Truhlar, Adv. Ser. Phys. Chem. **17**, 375 (2011).
[26]W. B. Tzeng, Y. R. Lee, and S. M. Lin, Chem. Phys. Lett. **227**, 467 (1994).
[27]W. S. McGivern, R. Li, P. Zou, and S. W. North, J. Chem. Phys. **111**, 5771 (1999).
[28]P. Zou, W. S. McGivern, and S. W. North, Phys. Chem. Chem. Phys. **2**, 3785 (2000).
[29]S.-H. Lee, Y.-J. Jung, and K.-H. Jung, Chem. Phys. **260**, 143 (2000).
[30]J. Zhou, K.-C. Lau, E. Hassanein, H. Xu, S.-X. Tian, B. Jones, and C. Y. Ng, J. Chem. Phys. **124**, 034309 (2006).
[31]N. H. Damrauer and G. Gerber, ACS Symp. Ser. **821**, 190 (2002).
[32]N. H. Damrauer, C. Dietl, G. Krampert, S.-H. Lee, K.-H. Jung, and G. Gerber, Eur. Phys. J. D **20**, 71 (2002).
[33]D. Irimia and M. H. M. Janssen, J. Chem. Phys. **132**, 234302 (2010).
[34]T. Takayanagi and A. Yokoyama, Bull. Chem. Soc. Jpn. **68**, 2225 (1995).
[35]T. Rozgonyi, T. Feurer, and L. González, Chem. Phys. Lett. **350**, 155 (2001).
[36]T. Rozgonyi and L. González, J. Phys. Chem. **106**, 11150 (2002).
[37]T. Rozgonyi and L. González, J. Phys. Chem. A **110**, 10251 (2006).
[38]T. Rozgonyi and L. González, J. Phys. Chem. A **112**, 5573 (2008).
[39]T. Rozgonyi and L. González, Chem. Phys. Lett. **459**, 39 (2008).
[40]T. Rozgonyi and L. González, J. Mod. Optics **56**, 790 (2009).
[41]J. Finley, P.-Å. Malmqvist, B. O. Roos, and L. Serrano-Andrés, Chem. Phys. Lett. **288**, 299 (1998).
[42]H. Nakano, J. Chem. Phys. **99**, 7983 (1983).
[43]C. A. Mead, J. Chem. Phys. **125**, 204109 (2006).
[44]N. L. Allinger, Y. H. Yuh, and J.-H. Lii, J. Am. Chem. Soc **111**, 8551 (1989).
[45]J.-Y. Shim, N. L. Allinger, and J. P. Bowen, J. Phys. Org. Chem. **10**, 3 (1977).
[46]J. W. Ponder, *TINKER v4.2* (Washington University, St. Louis, 2004). See the web site at http://dasher.wustl.edu/tinker.
[47]C. A. Piety, R. Soller, J. M. Nicovich, M. L. McKee, and P. H. Wine, Chem. Phys. **231**, 155 (1998).
[48]S. Enami, T. Yamanaka, S. Hashimoto, M. Kawasaki, and K. Tonokura, J. Phys. Chem. A **109**, 6066 (2005).
[49]J. J. Orlando, C. A. Piety, J. M. Nicovich, M. L. McKee, and P. H. Wine, J. Phys. Chem. A **109**, 6659 (2005).
[50]T. J. Gravestock, M. A. Blitz, and D. E. Heard, J. Phys. Chem. A **112**, 9544 (2008).
[51]R. Wada, R. C. Sharma, M. A. Blitz, and P. W. Seakins, Phys. Chem. Chem. Phys. **11**, 10417 (2009).
[52]S. L. Carrier, T. J. Preston, M. Dutta, A. C. Crowther, and F. F. Crim, J. Phys. Chem. A **114**, 1548 (2010).
[53]T. J. Preston, M. Dutta, B. J. Esselman, A. Kalume, L. George, R. J. McMahon, S. A. Reid, and F. F. Crim, J. Chem. Phys. **135**, 114503 (2011).
[54]S. Bailleux, P. Dréan, Z. Zelinger, and M. Godon, J. Mol. Spectrosc. **229**, 140 (2005).
[55]E. S. Whitney, T. Haeber, M. D. Schuder, A. C. Blair, and D. J. Nesbitt, J. Chem. Phys. **125**, 054303 (2006).
[56]H. Ozeki, T. Okabayashi, M. Tanimoto, S. Saito, and S. Bailleux, J. Chem. Phys. **127**, 224301 (2007).
[57]D. Bonhommeau and D. G. Truhlar, J. Chem. Phys. **129**, 014302 (2008).
[58]D. Bonhommeau, R. Valero, D. G. Truhlar, and A. W. Jasper, J. Chem. Phys. **130**, 234303 (2009).
[59]M. D. Hack, A. W. Jasper, Y. L. Volobuev, D. W. Schwenke, and D. G. Truhlar, J. Phys. Chem. A **103**, 6309 (1999).
[60]Z. H. Li, A. W. Jasper, D. A. Bonhommeau, R. Valero, and D. G. Truhlar, ANT–version 2012, University of Minnesota; http://comp.chem.umn.edu/ant.
[61]See supplementary material at http://dx.doi.org/10.1063/1.4747704 for the molecular mechanics equations and parameters.